

LA-UR-04-5132

Approved for public release;
distribution is unlimited.

Title:

IMPLEMENTATION OF ROOFTOP RECIRCULATION
PARAMETERIZATION INTO THE QUIC FAST RESPONSE
URBAN WIND MODEL

Author(s):

Nilesh Bagal
Balwinder Singh
Eric R. Pardyjak
Michael J. Brown



Submitted to:

5th AMS Urban Environment Conference
Vancouver, B.C.
Aug. 23-26, 2004



Los Alamos National Laboratory, an affirmative action/equal opportunity employer, is operated by the University of California for the U.S. Department of Energy under contract W-7405-ENG-36. By acceptance of this article, the publisher recognizes that the U.S. Government retains a nonexclusive, royalty-free license to publish or reproduce the published form of this contribution, or to allow others to do so, for U.S. Government purposes. Los Alamos National Laboratory requests that the publisher identify this article as work performed under the auspices of the U.S. Department of Energy. Los Alamos National Laboratory strongly supports academic freedom and a researcher's right to publish; as an institution, however, the Laboratory does not endorse the viewpoint of a publication or guarantee its technical correctness.

Form 836 (8/00)



N. Bagal¹, B. Singh¹, E. R. Pardyjak¹ and M. J. Brown²¹University of Utah, ²Los Alamos National Laboratory

1. INTRODUCTION

The QUIC (Quick Urban & Industrial Complex) dispersion modeling system has been developed to provide high-resolution wind and concentration fields in cities. The fast response 3D urban wind model QUIC-URB explicitly solves for the flow field around buildings using a suite of empirical parameterizations and mass conservation. This procedure is based on the work of Röckle (1990).

The current Röckle (1990) model does not capture the rooftop recirculation region associated with flow separation from the leading edge of an isolated building. According to Banks et al. (2001), there are two forms of separation depending on the incident wind angle. For an incident wind angle within 20° of perpendicular to the front face of the building, "bubble separation" occurs in which cylindrical vortices whose axis are orthogonal to the flow are generated along the rooftop surface (see Fig. 1). For a "corner wind" flow or incident wind angle of 30° to 70° of perpendicular to the front face of the building, "conical" or "delta wing" vortices form along the roof surface (Fig. 3).

In this work, a model for rooftop recirculation is implemented into the QUIC-URB model for the two incident wind angle regimes described above. The parameterizations for the length and height of the recirculation region are from Wilson (1979) for the case of flow perpendicular or near perpendicular to the building and from Banks et al. (2000) for the case of off-angle flow. In this paper, we describe the rooftop algorithms and show how the model results are improved through comparisons to experimental data (Snyder and Lawson 1994).

2. ROOFTOP RECIRCULATION FOR PERPENDICULAR OR NEAR PERPENDICULAR INCIDENT WIND ANGLES

On buildings with flat roofs and sharp edges, separation of the incident flow occurs at the leading edge of the roof. According to Wilson (1979), the flow separates from the upwind edge of the roof, and reattaches to the roof if the

building is long enough in the flow direction. The negative pressure gradient on the roof due to separation forms the recirculation region. The flow at roof level moves in the upwind direction in this recirculation cavity (Fig. 1). The smaller of the front face building dimensions (e.g., height or width) dominates the flow pattern of the rooftop recirculation. The flow takes the minimum resistant path to flow over the obstacle.

According to Wilson (1979), the length (L_c) and height (H_c) parameters for the rooftop recirculation region depend on the cross-stream geometry of the building and are given with respect to a scaling parameter (R) as follows:

$$R = B_S^{0.67} * B_L^{0.33}$$

$$H_c \text{ (Height of vortex)} = 0.22 * R$$

$$L_c \text{ (Length of vortex)} = 0.9 * R$$

B_S = Smaller of upwind building height or width.

B_L = Larger of upwind building height or width.

The notation for (H_c) has been modified from the original Wilson (1979) parameterization to facilitate implementation in QWIC-URB as shown in Fig. 1 below. In particular,

$$H_{CM} = H_c / 2$$

An ellipsoidal recirculation region has been implemented above the rooftop into the QUIC-URB model with the above length and height parameters. This ellipsoidal region represents the recirculation cavity as shown in Figure 1.

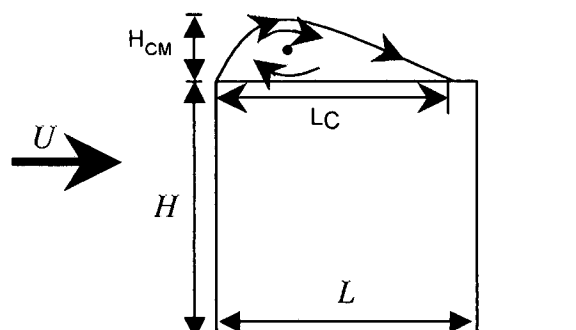


Fig. 1: Flow pattern above a rooftop indicating the Wilson (1979) parameters. U is the incident wind perpendicular to the building face. H_{CM} is the height and L_C is the length of the recirculation cavity.

* Corresponding author address: Nilesh L. Bagal, University of Utah, Department of Mechanical Engineering, Salt Lake City, UT 84112, e-mail: u0329233@utah.edu

In the new QUIC-URB rooftop recirculation algorithm, the ellipsoidal region is divided into two regions as shown in Figure 2:

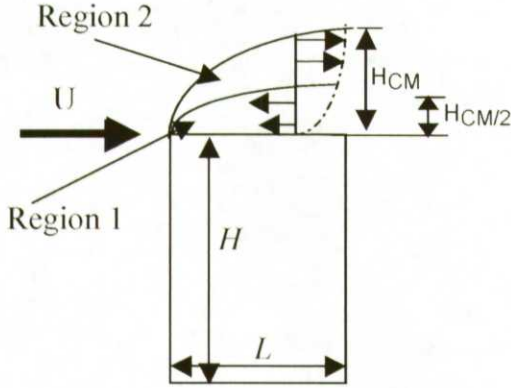


Fig. 2: Schematic of the rooftop recirculation region over a rectangular obstacle for the initial wind field in the QUIC-URB model. A negative logarithmic velocity vector with modification is implemented in Region 1, while a positive logarithmic profile is implemented in Region 2.

The ellipsoid defined by "Region 1" has a height that is one half of the total recirculation height H_{CM} . A logarithmic profile is implemented in the total ellipsoidal region and then in "Region 1" the logarithmic profile is reversed, i.e., the sign of the U component of velocity is changed. This element needs to be explicitly added in the QWIC-URB model to get the rooftop recirculation cavity, as the model only solves for mass consistency. The velocity in this reverse flow region is multiplied by a factor C_1 (Eq. 1) which is a function of the aspect ratio of the building where W is the width and H is the height of the building. The modified logarithmic velocity profile in "Region 1" is as given by Eq. 2 where K is the Von Karman constant, U_* is the friction velocity, Z_o is the roughness length and z is the vertical distance from the ground. The parameter C_1 effectively increases or decreases the wind magnitude in the rooftop cavity as a function of the upwind cross sectional geometry of the building. This parameter C_1 was obtained by minimizing the error with respect to the experimental data (Snyder and Lawson, 1994) for a cube.

$$C_1 = 1 + 0.05 \left(\frac{W}{H} \right) \quad (1)$$

$$\frac{U}{U_*} = \left(\frac{1}{K} \log \left(\frac{Z - H}{Z_o} \right) \right) C_1 \quad (2)$$

Finally mass conservation is applied to get the final wind field.

3. ROOFTOP RECIRCULATION FOR OFF-ANGLE (NON-PERPENDICULAR) INCIDENT WIND ANGLES

The capacity to incorporate the effects of non-orthogonal incident wind angles on rooftop flow has been added in the modified QUIC-URB model. In off-angle flows, a "delta wing" type vortex forms on the rooftop with a core that is not perpendicular to the incident wind angle (Banks et al. 2000) as shown in Figure 3.

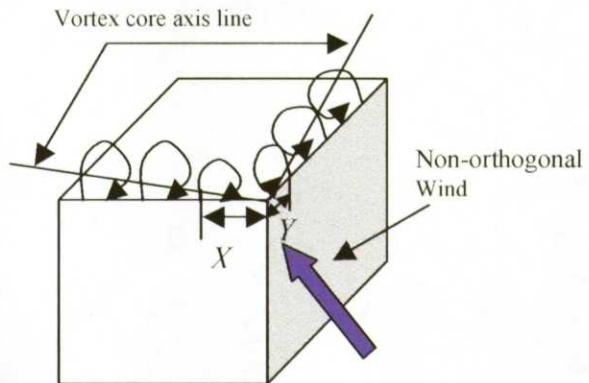


Fig. 3: Schematic of conical "delta-wing" corner vortices for a non-perpendicular incident wind angle, adapted from Banks et al. (2000).

The vortex is specified using a parameterization based on an empirical model by Banks et al. (2000). The length (L_c) and height (H_{cm}) of the vortex are calculated from the vortex core angle (ϕ_c), formed from the vortex core axis line and the leading edge of the roof, as shown in Figure 4.

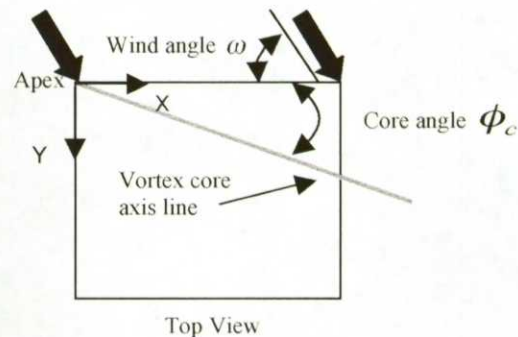


Fig. 4: Schematic showing the Vortex position nomenclature for a non-perpendicular incident wind angle (Banks et al. 2000).

Banks et al. (2000) performed experiments for varying incident wind angles to get a relation for incident wind angle (ω) with respect to vortex core angle (ϕ_c) which is valid for an incident wind angle of 30° to 70° . The relation is given in Eq. 3:

$$\phi_c = 2.94e^{0.0297\omega} \quad (3)$$

The height and length of the vortex region in x and y direction is defined as a function of the incident wind angle as given in Eq. 4 and 5 respectively:

$$L_{cx} = H_{cmx} = 2X \tan(\phi_c) \quad (4)$$

$$L_{cy} = H_{cmy} = 2Y \tan(\phi_c) \quad (5)$$

Where X and Y are the distances from the apex of the rooftop edge of the building as shown in Figure 3.

As in the perpendicular incident wind angle case, a vortex region is defined which is H_{cm} . A logarithmic profile is implemented throughout the depth of the vortex region and is then reversed in sign in the lower half of the region. At each grid location in the inner vortex region of the "delta wing vortex" a single initial velocity parameter (either U or V) is specified in the initial wind field for the model. The velocity (either U or V) is determined at each grid point by specifying it as the un-obstructed velocity magnitude as given by Eq. 6 and 7. It is then multiplied with the same factor C_1 as given in Eq. 1.

$$U(z) = \left[U(z)_{Upstream}^2 + V(z)_{Upstream}^2 \right]^{1/2} C_1 \quad (6)$$

$$V(z) = \left[U(z)_{Upstream}^2 + V(z)_{Upstream}^2 \right]^{1/2} C_1 \quad (7)$$

The initial wind field that is implemented in the model is shown in Figure 5.

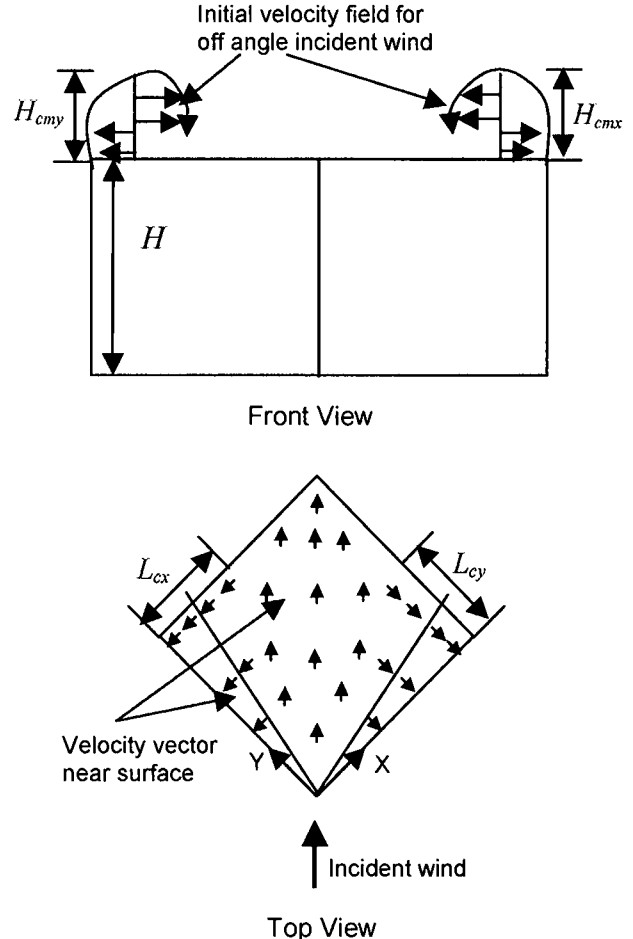


Fig. 5: Schematic of the initial wind field for an incident wind angle of 45° in the QUIC-URB model.

As above, the final wind field is obtained after mass consistency is enforced.

4. QUALITATIVE RESULTS

QUIC-URB-computed wind fields are plotted below for two different cases of incident wind direction. For inflow wind perpendicular to the building face, vector plots for a cube ($W=H=L$), a wide building ($W=10H$), and a long building ($L=2H$) are plotted (Figures 6, 7, and 8, respectively). Figure 7 is the vector plot for experimental data (Snyder and Lawson 1994) and the model computed velocity vector for a wide building ($W=10H$). As can be seen from the figure the new parameterization reproduces the size of the rooftop recirculation cavity fairly well when compared with the experimental data. In all the figures separation from the leading edge of the building can be seen. Reattachment of the rooftop cavity can be seen clearly in the case of the long building (Fig. 8).

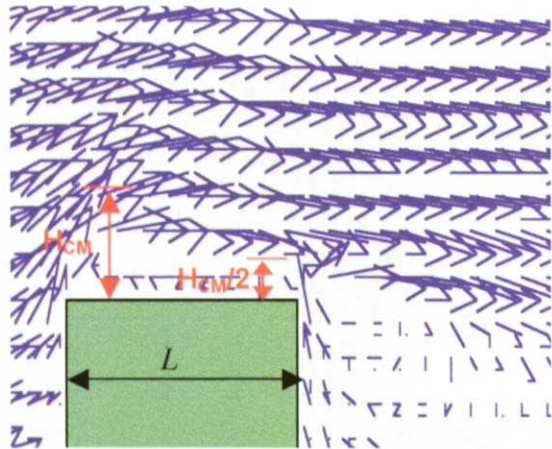


Fig. 6: Velocity vector plot for a cubic building ($W=H=L$) along the x-z center plane for incoming flow perpendicular to the building.

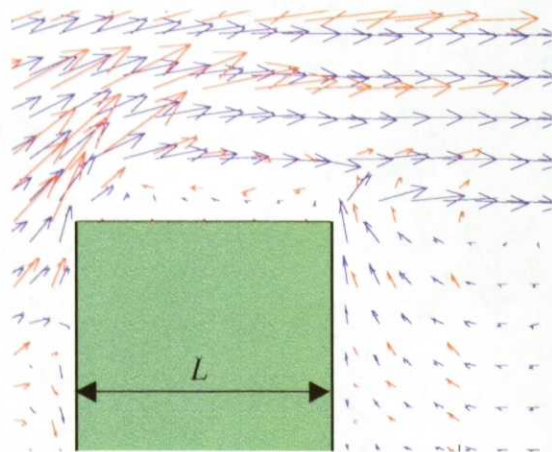


Fig. 7: Velocity vector plot with experimental data (Snyder and Lawson, 1994) (→) and model computed wind field (→) for a wide building ($W=10H$) along the x-z center plane for incoming flow perpendicular to the building.

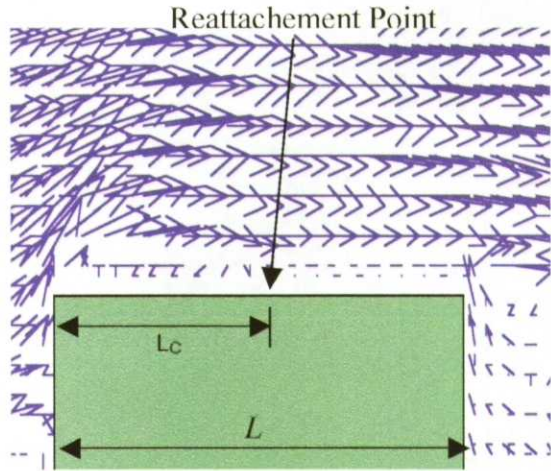
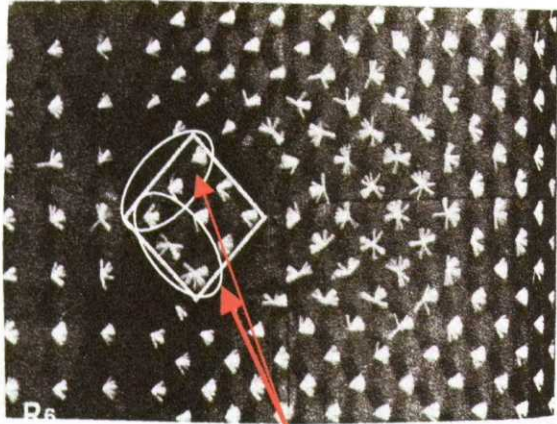


Fig. 8: Velocity vector plot for a long building ($L=2H$) along the x-z center plane for incoming flow perpendicular to the building.

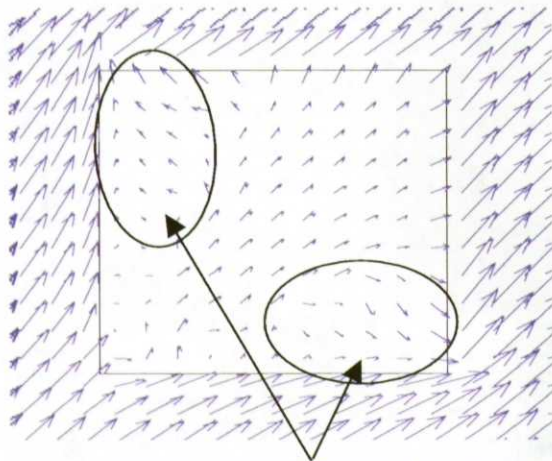
Figure 9 is a rooftop vane flow visualization study done by Ogawa et al. (1983) for an incident wind angle of 45° . In the figure the cube is outlined by a white line and the free stream flow is from left to right. As can be seen in the figure for the rooftop a “delta wing vortex” is formed along the leading edge of the building. The velocity vector is perpendicular to the corresponding building edge as marked in the figure.

For a 45° incident wind angle, velocity vectors are plotted for an x-y plane in Figures 10 and 11. Figure 10 shows a plane above the rooftop ($z/H = 1.1$) for flow above a cube ($W=H=L$). As marked in the figure, the reversed velocities which are almost perpendicular to the corresponding leading edge of the building of the “delta wing vortex” can be seen. Figure 11 shows another plane above the rooftop ($z/H = 1.2$) in which the velocities in the “delta wing vortex” follow the free stream velocity field.



Near surface vane showing the flow pattern associated with "delta wing" vortex

Fig. 9: Model vane flow visualization study by Ogawa et al. (1983). The building is outlined in white. The visualization shows the vortex formed along the rooftop leading edge for an incident wind angle of 45°.



Velocity vector showing the flow pattern associated with "delta wing" vortex

Fig. 10: X-Y plane velocity vector plot for a cube ($W=H=L$) with a cornering incident wind angle (45°) at $z/H = 1.1$

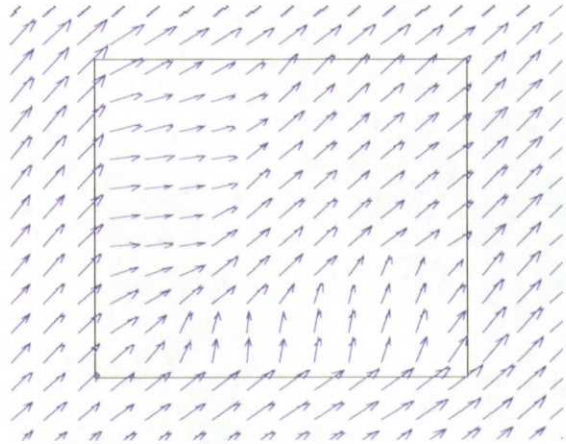


Fig. 11: X-Y plane velocity vector plot for a cube ($W=H=L$) with a cornering incident wind angle (45°) at $z/H = 1.2$

Qualitatively the results from the QUIC-URB model as shown in Figures 10 and 11 seem to agree with the flow pattern from the Banks et al. (2000) and Ogawa et al. (1983) flow visualization studies, however the model needs to be validated with the experimental data more thoroughly.

5. DIRECT EXPERIMENT COMPARISONS

To test the new rooftop recirculation model QUIC-URB results were compared to data collected in the wind tunnel at the U.S. Environmental Protection Agency's Fluid Modeling Facility (Snyder and Lawson, 1994) for a cube ($W=H=L$), a relatively wide building ($W=10H$) and a long building ($L=2H$) (Figures 12, 13 and 14, respectively). The power law exponent input parameter was set as 0.16 to match the experimental data. The inflow winds were perpendicular to the building model. QUIC-URB results were computed using the new rooftop recirculation scheme and the original Röckle (1990) model for comparison. The grid resolution for the model was set to 1 meter/grid to validate with the experimental data. Figures 12, 13 and 14 show the vertical profiles of normalized velocity $u/U(H)$ for QUIC-URB with the recirculation scheme (---), QUIC-URB with no recirculation scheme (-), and the experimental measurements (o). The center of the building is located at $x/H = 0$ and the building extends through $z/H = 1$ in the plots. The stream wise extent of the building was from $x/H = -0.5$ to $x/H = 0.5$ for Figures 12, 13 and from $x/H = -0.75$ to $x/H = 0.75$ Figure 14. The computed velocities using the new recirculation scheme clearly match the experimental data better. Figure 12 shows that the size of the recirculation cavity matches the data,

also the normalized velocity magnitude follow the experimental data well. Figure 13 shows that the depth of the recirculation cavity is underestimated for the wide building ($W=10H$), nevertheless the cavity size parameterization implemented confer minimum error for all geometry cases. As can be

seen from Figure 14, the reattachment point is at $x/H=0$ for the modified model as well as the experimental data. There is a 30% reduction in the error values between the computed velocity field and the experimental data when compared with the original Röckle (1990) model.

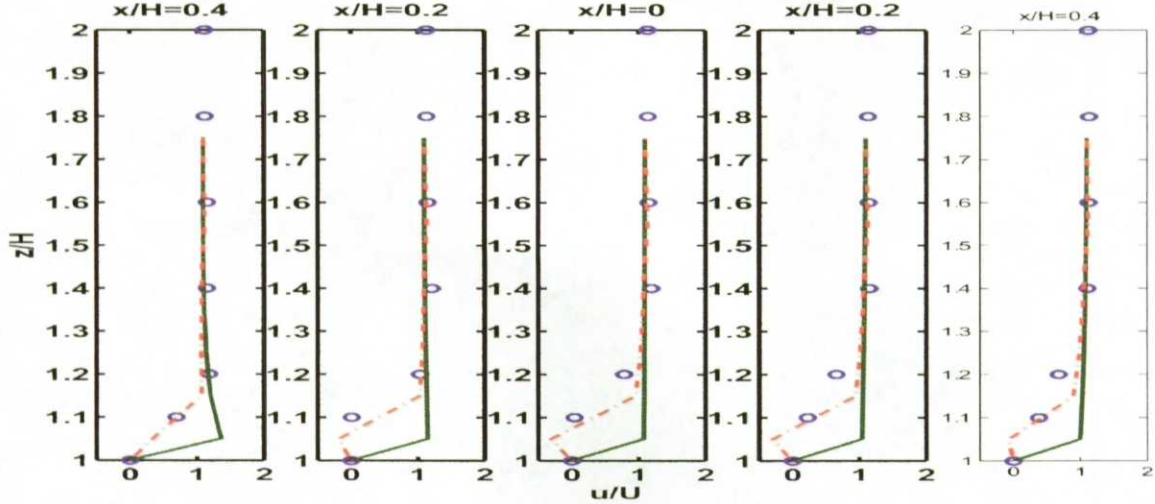


Fig. 12: Comparison of normalized streamwise velocity above the rooftop for experimental measurements of Snyder and Lawson (1994) (o) and for QUIC-URB with (---) and without (-) rooftop recirculation for a cube ($W=H=L$).

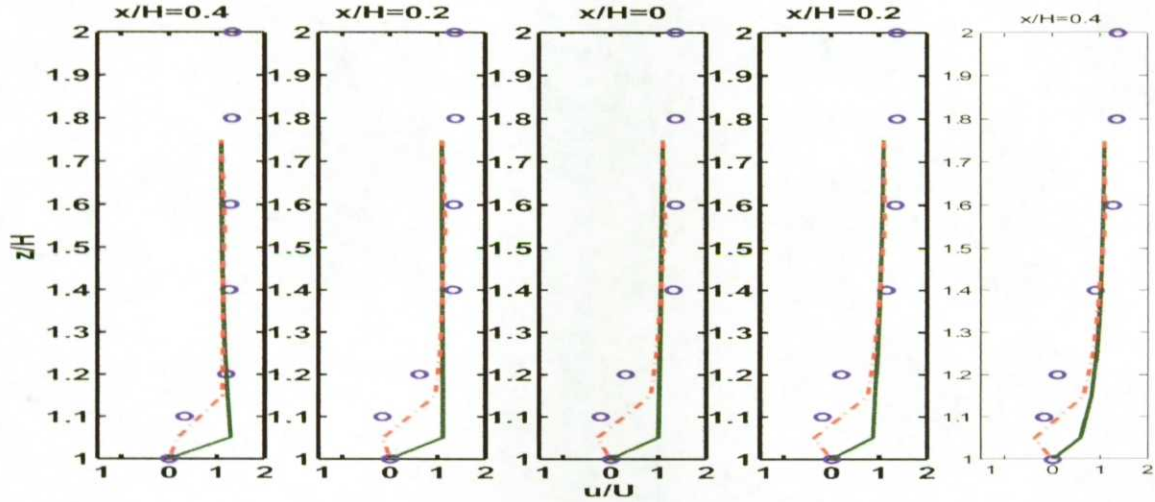


Fig. 13: Comparison of normalized streamwise velocity above the rooftop for experimental measurements of Snyder and Lawson (1994) (o) and for QUIC-URB with (---) and without (-) rooftop recirculation for a wide building ($W=10H$).

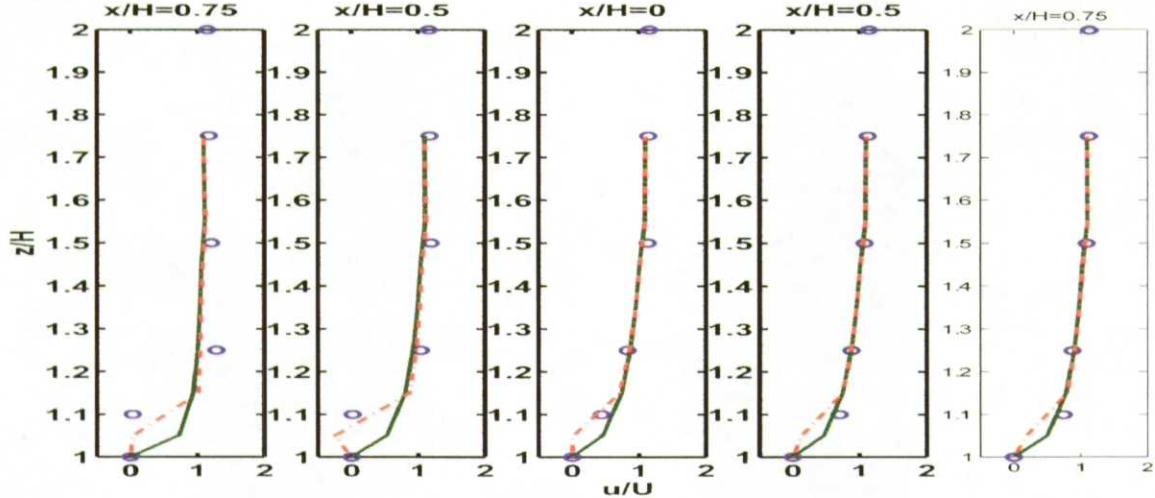


Fig. 14: Comparison of normalized streamwise velocity above the rooftop for experimental measurements of Snyder and Lawson (1994) (o) and for QUIC-URB with (--) and without (-) rooftop recirculation for a long building ($L=2H$).

6. SUMMARY

In this work, a rooftop recirculation model was incorporated into the 3D fast response urban wind model QUIC-URB. The rooftop recirculation cavity length parameterization was implemented in the model for perpendicular incident wind angles following Wilson's (1979) parameterization and for non-orthogonal incident flow angles following the parameterization of Banks et al. (2000). The model-experiment comparison for a cube, wide building, and long building in the case of flow perpendicular to the building face show that the suggested parameterization is justified as it matches experimental data quite well. The velocity parameterization in the cavity region is derived from matching the experimental data for a cubical building. The constants give the minimum error for model-experiment comparisons in all geometry cases. The non-orthogonal wind angle parameterization still needs to be evaluated using experimental data, however the qualitative agreement with the flow visualization study by Banks et al. (2000) and Ogawa et al. (1983) appears to be reasonable. The model will be compared to the available Ogawa et al. (1983) and Leitl (2000) data sets. In addition grid resolution studies will be performed to test the sensitivity of the model.

7. REFERENCES

Banks, D., R.N. Meroney, P.P. Sarkar, Z. Zhao, and F. Wu, 2000: Flow visualization of conical vortices on flat roofs with simultaneous surface pressure measurement. *Journal of Wind Engineering and Industrial Aerodynamics*, **84**, 65-85.

Banks, D., and R.N. Meroney, 2001 (a): A Model Of roof-top surface pressures produced by conical vortices: Evaluations and implications. *Wind and Structures*, **4**, 279-298.

Banks, D., and R.N. Meroney, 2001 (b): The applicability of quasi-steady theory to pressure statistics beneath rooftop vortices. *Journal of Wind Engineering and Industrial Aerodynamics*, **89**, 569-598.

Leitl, B., 2000: Validation data for micro scale dispersion modeling. *EUROTRAC - Newsletter*, **22**, 28-32.

Ogawa, Y., S. Oikawa, and K. Uehara, 1983: Field and wind tunnel study of the flow and diffusion around a model cube-1. Flow measurements. *Atmospheric Environment*, **17**, 1145-1159.

Röckle, R., 1990: Bestimmung der Stomungsverhältnisse im Bereich Komplexer Bebauungsstrukturen. Ph.D. thesis, *Vom Fachbereich Mechanik, der Technischen Hochschule Darmstadt*, Germany.

Snyder, W.H., and R.E. Lawson, 1994: Wind-tunnel measurements of flow fields in the vicinity of buildings. *8th Joint Conf. on Applic. of Air Poll. Meteor. with AWMA*, Nashville, TN, Amer. Meteor. Soc., 23-28.

Wilson, D. J., 1979: Flow pattern over flat-roofed buildings and application to exhaust stack design. *ASHRAE*, **85**, 284-295